Coastal Dynamics 2017
Paper No. 165

A NUMERICAL INVESTIGATION OF SHEET FLOW UNDER NON-BREAKING AND BREAKING WAVES

Yeulwoo Kim[1], Zhen Cheng[2], Tian-Jian Hsu[1], Ryan S. Mieras[1] and Jack A. Puleo

Abstract

An Eulerian two-phase flow model for sediment transport, SedFoam (Cheng et al., 2017), is fully coupled with the surface wave model, waves2Foam (Jacobsen et al., 2011). The resulting solver, SedWaveFoam, can simulate sediment transport under surface wave propagation without artificial matching between the surface wave field and bottom boundary layer sediment transport. SedWaveFoam is validated with measured sheet flow data driven by non-breaking monochromatic waves (Dohmen-Janssen and Hanes, 2002). Onshore transport rate is obtained similar to the measured data. The onshore transport rate is about two times larger than that obtained in a hypothetical oscillating water tunnel. Ongoing work uses the coupled model to simulate sheet flow measured under skewed/asymmetric waves over a surf zone sandbar (BARSED, Mieras et al., 2017).

Key words: sediment transport, sheet flow, wave-driven sediment transport, numerical modeling, OpenFOAM.

1. Introduction

Prediction of nearshore morphological evolution is of major importance to ensure the sustainability of coastal communities. However, predicting nearshore morphodynamics, particularly during major storms, has been a challenging topic due to difficulties in acquiring detailed flow characteristics and sediment dynamics in the thin bottom boundary layer. A comprehensive understanding of the complex mechanisms associated with wave-driven sediment transport remains incomplete, particularly regarding the relative importance among many interconnected processes, such as wave skewness, wave asymmetry and boundary layer streaming (e.g. Henderson et al., 2004; Ruessink et al., 2009; Yu et al., 2010). Conventionally, sediment transport rate driven by waves was estimated based on the concept of bed shear stress (Ribberink, 1998). A number of studies have revealed that that under strong bed shear stress, most of the transport occurs within the concentrated region in sheet flow (e.g. Horikawa et al., 1982; McLean et al., 2001; Ribberink and Al-Salem, 1994). In addition, horizontal pressure gradient is recognized as an important factor triggering momentary bed failure under steep waves (Madsen 1974; Sleath, 1999). Hence, parameterization of wave-induced sheet flow may require the combined effect from the bed shear stress, horizontal pressure gradient and boundary layer streaming (Anderson et al., *in review*; Cheng et al., 2017; Foster et al., 2006; van der A et al., 2013).

Many laboratory experiments (e.g. Dohmen-Janssen et al., 2001; O'Donoghue and Wright, 2004; Ribberink, 1998; Ribberink and Al-Salem, 1994) have been conducted to study sheet flow in large oscillating water tunnels (OWTs, also called U-tubes). Oscillatory flows of the order of $u = \mathrm{O}(1)$ m/s and $T = \mathrm{O}(10)$ s can be generated in such OWTs, and hence a dynamic scaling effect can be minimized. Ribberink and Al-Salem (1994) showed that the mobile bed and sediment affect turbulence intensity in the oscillatory boundary layer. In addition, bed-load based transport formula obtained from steady flows requires modification for oscillatory flows due to changes in effective roughness and turbulence modulation (Dohmen-Janssen et al., 2001; Ribberink, 1998). On the other hand, intergranular interaction increases flow resistance in the sheet flow layer, depending on the grain size (Dohmen-Janssen et al., 2001). As a result, typical fixed-bed single-phase boundary layer models may not be appropriate for

[1]Coastal Engineering Laboratory, Department of Civil and Environmental Engineering, University of Delaware, Newark, DE, USA. ykim@udel.edu
[2]Applied Ocean Physics and Engineering, Woods Hole Oceanographic Institution (WHOI), Woods Hole, MA, USA.

modeling sheet flow.

The main limitation in OWT experiments is the lack of realistic surface wave effects. Dohmen-Janssen and Hanes (2002) reported detailed measurements of sheet flow under non-breaking surface waves. They found a significant difference in net sediment transport rate and sheet layer thickness between OWT and wave flume experiments under the same maximum non-dimensional bed shear stress. A modified Meyer-Peter and Müller type (Meyer-Peter and Müller, 1948) transport model was applied (Nielsen, 2006; Nielsen and Callaghan, 2003) to account for the increased net transport rate under the real waves. The results indicated that wave-induced boundary layer streaming is an important factor causing the increased net sediment transport rate. An enhanced sheet flow thickness was also observed under strongly skewed-asymmetric waves on a sandbar crest (Mieras et al., *in review*). Therefore, a numerical model which can resolve the evolution of free surface and the resulting wave field, wave-induced boundary layer, and wave-driven sheet flow transport is needed for predicting nearshore sediment transport.

Motivated by this need, sediment transport under periodic waves for flat bottom and barred beach conditions are investigated by coupling an Eulerian two-phase flow model, SedFoam (Cheng et al., 2017), with a volume-of-fluid (VOF) solver, InterFoam (Berberovic´ et al., 2009) facilitated by a comprehensive wave generation/absorption toolbox, waves2Foam (Jacobsen et al., 2011). SedFoam resolves the full vertical profile of sediment transport using the Reynolds-averaged Eulerian two-phase flow equations with closures of inter-granular stresses and a k-ε turbulence model. The wave generation toolbox, waves2Foam, designed to work with InterFoam, can generate/absorb various type of surface waves. The fully coupled model, named SedWaveFoam, can be used to simulate the effect of wave-induced bottom shear stress, pressure gradients, boundary layer streaming, and wave-breaking turbulence on the full vertical profiles of sediment transport without conventional bedload/suspended load assumptions. As a first step, the model is validated for sheet flow under non-breaking monochromatic waves (Dohmen-Janssen and Hanes, 2002). The coupled model is then applied to the sandBAR SEDiment transport experiment (BARSED; Anderson et al., *in review*; Mieras et al., *in review*) data to study the effects of steep waves on sheet flow processes.

2. Numerical Model

The numerical model is based on coupling/merging several existing solvers in the open-source CFD toolbox, OpenFOAM. For the air and water phases, the flow is solved by InterFoam (Berberovic´ et al., 2009), which tracks the interfaces of two incompressible fluids. Particularly, the water-air interfaces are computed by tracking the volumetric concentration of the water phase, similar to the well-known volume-of-fluid method (Hirt and Nichols, 1981). Jacobsen et al. (2011) enhanced this solver with a comprehensive surface wave generation/absorption scheme and the resulting solver, called waves2Foam, has been applied to study surf zone processes (e.g. Jacobsen et al., 2014). In the past decade, the Eulerian two-phase flow formulations have been widely used to model sediment transport in sheet flow condition (e.g. Dong and Zhang, 2002; Hsu et al. 2004). Recently, A multi-dimensional two-phase flow model for sediment transport, called SedFoam (Cheng et al., 2017), was developed using OpenFOAM. The SedFoam model was validated with measured data for several oscillatory sheet flow data sets reported by O'Donoghue and Wright (2004) (see also Section 3). Combining these two solvers to a new solver for wave-induced sediment transport applications becomes less difficult under the framework of OpenFOAM.

The governing equations of this new two-phase flow solver for wave-induced sediment transport are briefly presented. The mass conservation equations for the mixture of carrier flow (water-air) phase and sediment phases are derived by assuming no mass transfer between the phases:

$$\frac{\partial \phi^s}{\partial t} + \frac{\partial \phi^s u_i^s}{\partial x_i} = 0 \tag{1}$$

$$\frac{\partial \phi^m}{\partial t} + \frac{\partial \phi^m u_i^m}{\partial x_i} = 0, \tag{2}$$

in which ϕ^s and ϕ^m are the volumetric concentration of the sediment and water-air mixture phases, respectively, with $\phi^m = \phi^{\text{water}} + \phi^{\text{air}}$ and $\phi^m + \phi^s = 1$. The variable u_i^s is the sediment velocity and u_i^m is the carrier fluid phase velocity which can be written as

$$u_i^m = \frac{\phi^{\text{water}} u_i^{\text{water}} + \phi^{\text{air}} u_i^{\text{air}}}{\phi^{\text{water}} + \phi^{\text{air}}} = u_i^{\text{water}} - \frac{\phi^{\text{air}} u_i^r}{\phi^{\text{m}}}, \tag{3}$$

where u_i^r represents the relative velocity between air and water, defined as $u_i^r = u_i^{\text{water}} - u_i^{\text{air}}$. The variable u_i^r is obtained by iteration using the interface compression method (Klostermann et al., 2012) to minimize the diffusion at the free surface while retaining computational efficiency. Equation (2) can be rewritten as

$$\frac{\partial \phi^{\text{water}}}{\partial t} + \frac{\partial \phi^{\text{water}} u_i^{\text{water}}}{\partial x_i} + \frac{\partial \dfrac{\phi^{\text{water}} \phi^{\text{air}}}{\phi^{\text{water}} + \phi^{\text{air}}} u_i^r}{\partial x_i} = 0. \tag{4}$$

The momentum equations are written as

$$\frac{\partial \rho^m \phi^m u_i^m}{\partial t} + \frac{\partial \rho^m \phi^m u_i^m u_j^m}{\partial x_j} = -\frac{\partial \phi^m p}{\partial x_i} + \rho^m \phi^m g \delta_{i3} + \frac{\partial \tau_{ij}^m}{\partial x_j} + M_i^{ms} \tag{5}$$

$$\frac{\partial \rho^s \phi^s u_i^s}{\partial t} + \frac{\partial \rho^s \phi^s u_i^s u_j^s}{\partial x_j} = -\frac{\partial \phi^s p}{\partial x_i} - \frac{\partial p^s}{\partial x_i} + \frac{\partial \tau_{ij}^s}{\partial x_j} + \rho^s \phi^s g \delta_{i3} + M_i^{sm}, \tag{6}$$

where $\rho^m = \left(\rho^{\text{water}} \phi^{\text{water}} + \rho^{\text{air}} \phi^{\text{air}}\right) / \phi^m$, ρ^s is the sediment density, p is the fluid pressure, and g is the gravitational acceleration. The fluid stress includes the sum of viscous and Reynolds tresses, calculated with a two-equation k-ε turbulence model derived for two-phase flow, in which sediment can attenuate flow turbulence via a range of mechanisms depending on the particle inertia (Cheng et al., 2017; Yu et al., 2010). The inter-phase momentum transfer between the carrier flow and sediment phases follows Newton's 3rd law, $M^{ms} = -M^{sm}$. Here, drag and buoyancy forces are considered. The particle normal stress, p^s, and shear stress, τ_{ij}^s, are modeled with kinetic theory of granular flow for moderate concentration. For high sediment concentration stress associated with enduring contact and frictional effect are incorporated. More details on model formulation and numerical implementation are given elsewhere (Cheng et al., 2017; Jacobsen et al., 2011; Klostermann et al., 2012).

3. Model Results

3.1. *Capability of individual model*

SedFoam was validated (Figure 1) with the measured concentration profile of medium sand (d = 0.28 mm) obtained under sinusoidal wave motion in an OWT with wave period $T = 7.5$ s and maximum velocity $U_{\max} = 1.26$ m/s (case 7515 in O'Donoghue and Wright, 2004). The concentration profiles at two different instants (identified by symbols in Figure 1a) were selected for comparison. Suspended sediment concentration is notably different between the wave crest (Figure 1b) and flow reversal (Figure 1c). Generally, good agreements with measured concentration and flow velocity (not shown) were obtained. More comprehensive model validation for other cases reported by O'Donoghue and Wright (2004), including velocity profiles and erosion depths are found in Cheng et al. (2017). A comprehensive understanding of sediment transport in nearshore environment cannot be achieved due to the lack of realistic influence from the free surface, although SedFoam is capable of predicting sediment transport

under oscillatory flow in OWTs. As a result, the capability of simulating the evolution of free surface and the resulting wave field were included in the model.

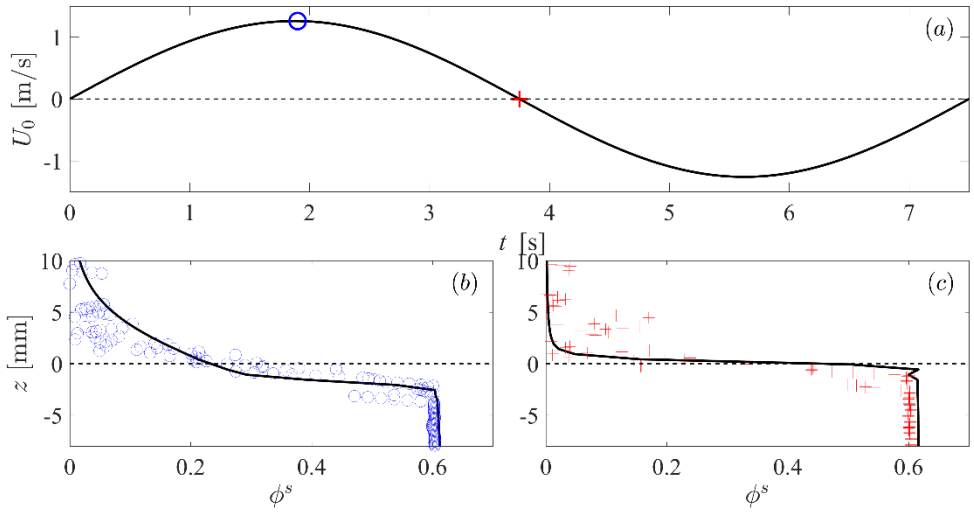

Figure 1. Model-data comparison of (a) time series of free-stream velocity at the wave crest and flow reversal: (b) t = 1.90 s; (c) t = 3.75 s. The corresponding comparison of sediment concentration profiles between the model results (solid lines) and measured data (symbols) at these two instants are shown in panels (b) and (c).

The BARSED experiment was carried out in the large-scale wave flume at O. H. Hinsdale Wave Research Laboratory, Oregon State University, USA. Waves2Foam was tested with the wave conditions of Trial 14 (S1T7H60) from the BARSED experiment (Figure 2). This trial had a wave period of 7.0 s and wave height of 0.66 m at the toe of the profile, and was chosen since it had the largest sheet layer thickness (Mieras et al., *in review*). The model domain was comprised of 1321, 43, 73 grid points in the streamwise (x), spanwise (y), and vertical (z) directions, respectively. The grid size in the streamwise and vertical directions was non-uniform, with a minimum size of 3 cm (in x) and 1 cm (in z). On the other hand, the grid size in the spanwise direction was uniformly 4 cm. Standard Smagorinsky closure was used for sub-grid viscosity. A total of 4.1 million grid points were used for this preliminary simulation. Twin-wire capacitance wave gauges were deployed at 18 cross-shore locations in BARSED (Figure 2a). The wave breaking occurred right on the sandbar crest in the model, consistent with the observations (Mieras et al., 2017). The temporal evolution of free-surface at the seaward-edge of the sandbar is also shown in Figure 2b. After about five wave periods, the free surface elevation reaches quasi-stationary state. Overall, the model is able to predict the free-surface elevation reasonably well. Based on the wave shape, a steep wave velocity is expected to drive bottom sediment transport although the breaking-wave-induced turbulence does not approach the bar crest for this particular trial.

3.2. *SedWaveFoam results*

The sheet flow experiment under monochromatic nonbreaking waves reported by Dohmen-Janssen and Hanes (2002) was simulated to test the newly developed solver SedWaveFoam. The detailed physical model setup and results were explained in Dohmen-Janssen and Hanes (2002), thus only a brief overview of the setup is discussed here. The sheet flow experiment was carried out in the large wave flume (GWK), in Hannover, Germany. The water depth at the measurement section (flat sand bed) was 3.5 m, elevated by 0.75 m relative to the bottom of the wave paddle (h = 4.25 m). The sand bed was constructed of well-sorted quartz with a median grain diameter of 0.24 mm. A multiple transducer array (MTA) was deployed to measure the bed level change. A conductivity concentration meter (CCM) system was installed under the sand bed to obtain sediment concentration in the concentrated region. Two sets of acoustic backscatter sensors (ABS) were used to measure the suspended sediment concentration. The velocity of the carrier fluid was measured using an acoustic doppler velocimeter (ADV) 0.109 m above the sand bed.

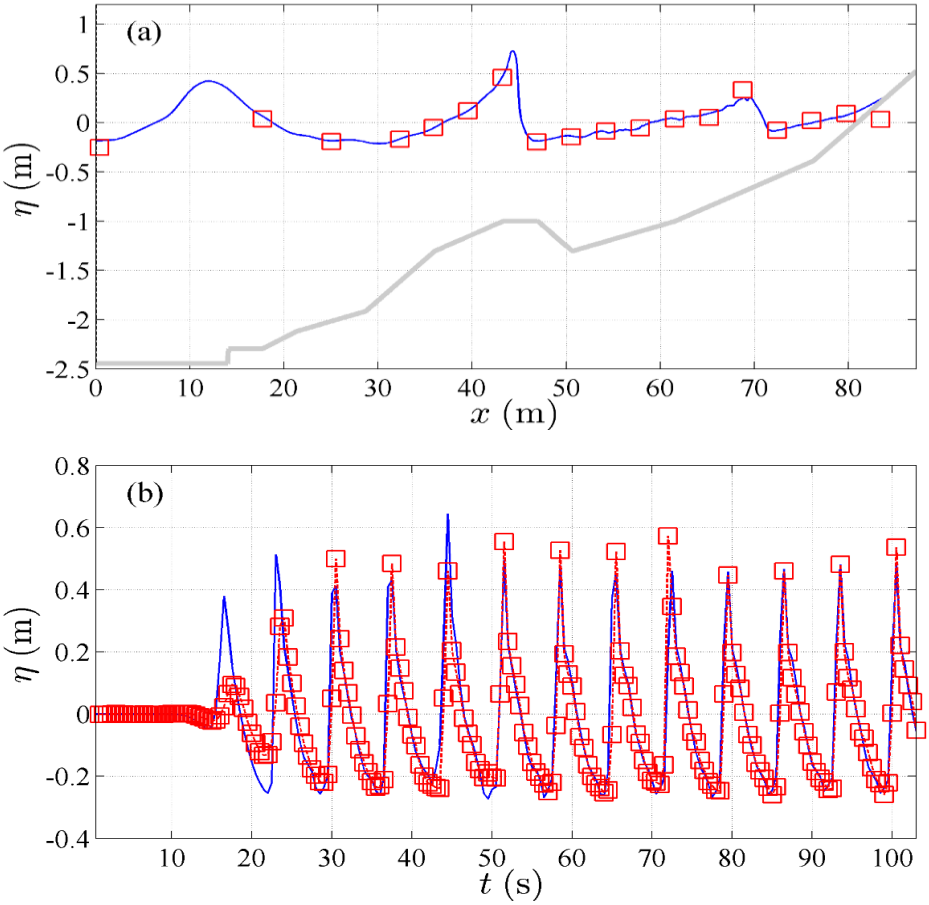

Figure 2. Measured (red symbols) and modeled (blue solid line) (a) profile of free-surface elevation at t = 86.5 s and (b) time series of free-surface elevation at the seaward-edge of the sandbar crest (x = 43.2 m).

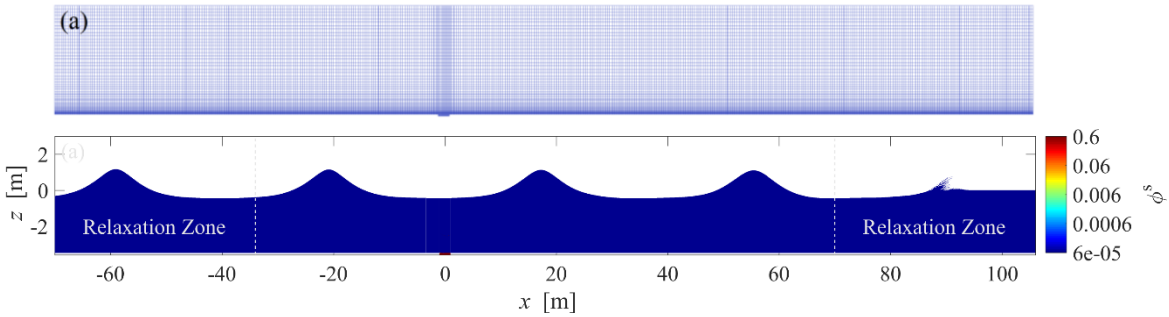

Figure 3. The numerical flume with (a) mesh (down-sampled) and (b) white surface (air phase), blue surface (water phase), and red surface at x = 0 m (sediment phase) based on the experiment setup (Dohmen-Janssen and Hanes, 2002). For visibility, vertical scale is stretched three times.

3.2.1. *Model setup*

The numerical model domain is a 2D flume that is 176 m long (~5 wave lengths, 5L) and 6.5 m deep with a water depth of 3.5 m (Figure 3). The sediment pit of 2 m long and 0.1 m deep was located 2L away from the inlet, consisted of the sand (d = 0.24 mm) with the maximum volumetric concentration of $\phi^s_{\max} = 0.61$ in the sediment bed. It should be noted that the model domain was simplified for computational efficiency

with only the flat portion of the flume in the physical experiment simulated. The model domain was comprised of 8,994 and 1,116 ~ 1,216 grid points in the streamwise (x) and vertical (z) directions, respectively. The grid size was non-uniform, with a minimum width of 1 cm and height of 1 mm near the pit while the grid size is 2 cm in width and 1 cm in height away from the pit. Hence, a total number of 10.1 million computational grid points was used for the simulation (Figure 3a).

Except for the top atmospheric boundary (open boundary condition) and side walls (empty condition in OpenFOAM), all other boundaries (bottom and ends) were specified as walls with no-flux boundaries for scalar quantities and velocity components normal to the wall. The wall-parallel velocity at the boundaries was set to 0 (no-slip). At each end of the wave flume, a relaxation zone of $1L$ was adopted for wave generation/absorption and to suppress reflected waves. In the present setup, the wave height of reflected waves was less than 10 % of incident wave height. Non-breaking monochromatic waves ($H = 1.6$ m, $T = 6.5$ s) were sent into the domain using 10th order stream function (Figure 3b).

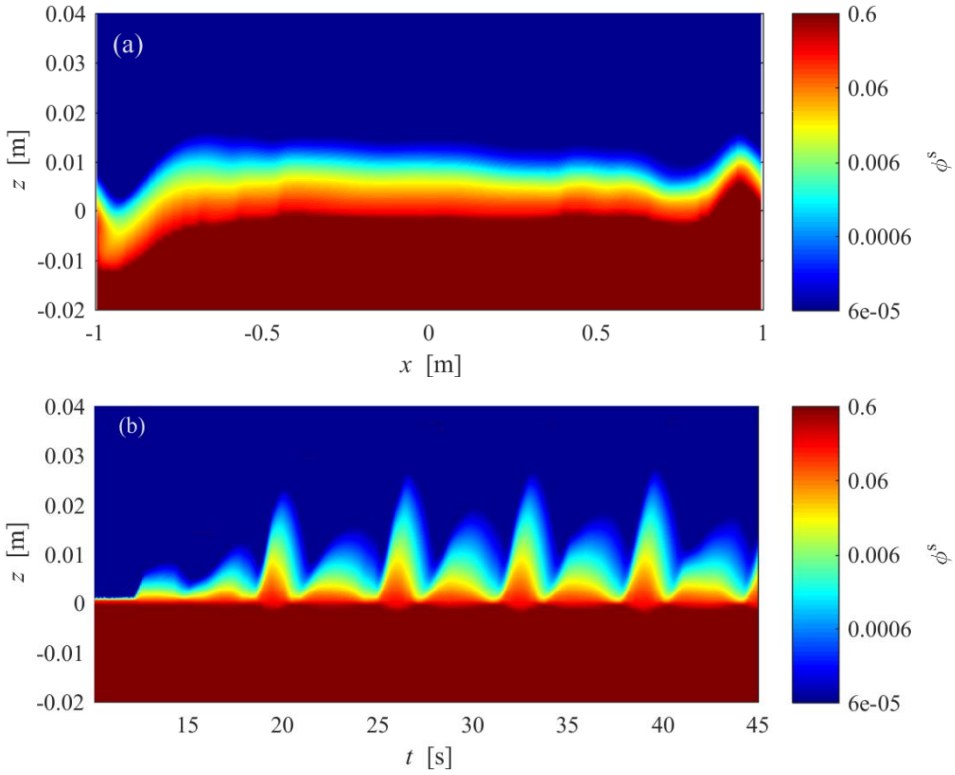

Figure 4. (a) A snapshot at $t = 45$ s for sediment concentration over the entire sand pit. (b) time series of volumetric concentration of sediment phase at the center ($x = 0$ m) of the sand pit.

3.2.2. *Model-data comparison*

The model can produce the expected temporal and spatial evolutions of sediment phase under the surface waves (Figure 4). For example, Figure 4a shows the x-z plane snapshot of the volumetric concentration of sediment at the selected instant (t = 45 s). Noticeable scour is observed at the left edge of the pit (Figure 4a), caused by the lack of sediment flux upstream from the pit. Similarly, notable accumulation of sediment is observed at the downstream edge of the pit. At the center of the pit ($x = 0$ m), a region of flatbed occurs. The time series of sediment phase at the center of the pit is presented in Figure 4b. After the passage of a couple of waves, the sediment concentration evolution has approximately reached a quasi-steady state, allowing the 5th wave (t = 37.7 ~ 44.2 s) to be further analyzed for the model-data comparison. The temporal evolution of free stream velocity for the 5th wave at $z = 0.109$ m above the bed in the center of the pit agrees reasonably well with measured data (Figure 5). Some discrepancies were found near the wave trough due to limited information of incident wave. The wave condition was only given at the wave paddle, hence several different types of incident waves (e.g. cnoidal wave) have been tested to better match the

forcing conditions.

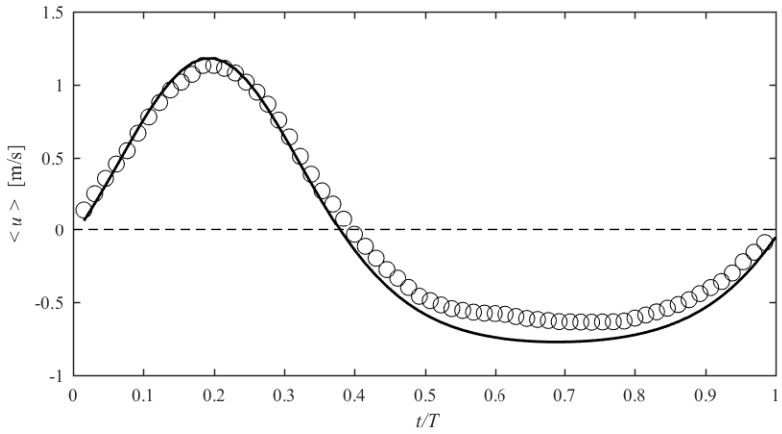

Figure 5. Time series of free stream velocity (measured data, symbols; model results, line) at z = 0.109 m in the center of the sand pit (x = 0 m).

The model-data comparison of wave-averaged (for the 5th wave) sediment concentration profile is presented in Figure 6. It should be reiterated that the maximum concentration reported in the physical experiment is 0.67 (Dohmen-Janssen and Hanes, 2002), which was slightly larger than the typical packing limit for uniform, spherical particles probably owing to mixed grain sizes in the sediments. The present model cannot account for the effect of mixed grains, and hence the modeled concentrations are simply multiplied by a factor of 0.67/0.61 for the remainder of model validations. The modeled sediment concentration agrees well with the measured data (measured by CCM, ○; Figure 6) in the moderate to highly concentrated region ($\phi_s > 10^{-2}$). However, the predicted concentration in the dilute region is less satisfactory (those measured by ABS, +; Figure 6). As demonstrated later, the model results suggest that the sediment flux within the bottom 10 mm ($\phi_s > 10^{-3}$) accounts for 99.8% of the total transport rate.

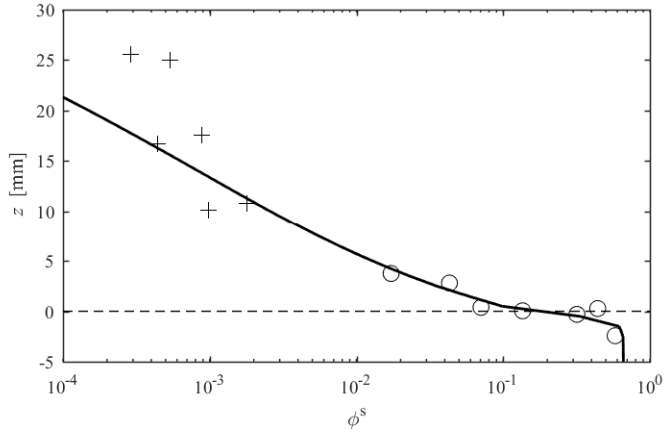

Figure 6. Wave-averaged sediment concentration profile between the measured data (CCM, ○; ABS, +) and model results (solid line).

Figure 7 shows the instantaneous sediment concentration profile in the sheet flow layer in the 5th wave cycle. Under the wave crest (Figure 7b) and trough (Figure 7d), the increase of sheet layer thickness is apparent compared to those during the flow reversals (Figure 7a and 7c). The model results indicate that the driving force of sheet flow is closely related to near-bed velocity (see Figure 5), consistent with the observation reported by Dohmen-Janssen and Hanes (2002). The agreement between the model results and measured data are good. Clearly, higher vertical numerical resolution is needed in the future runs.

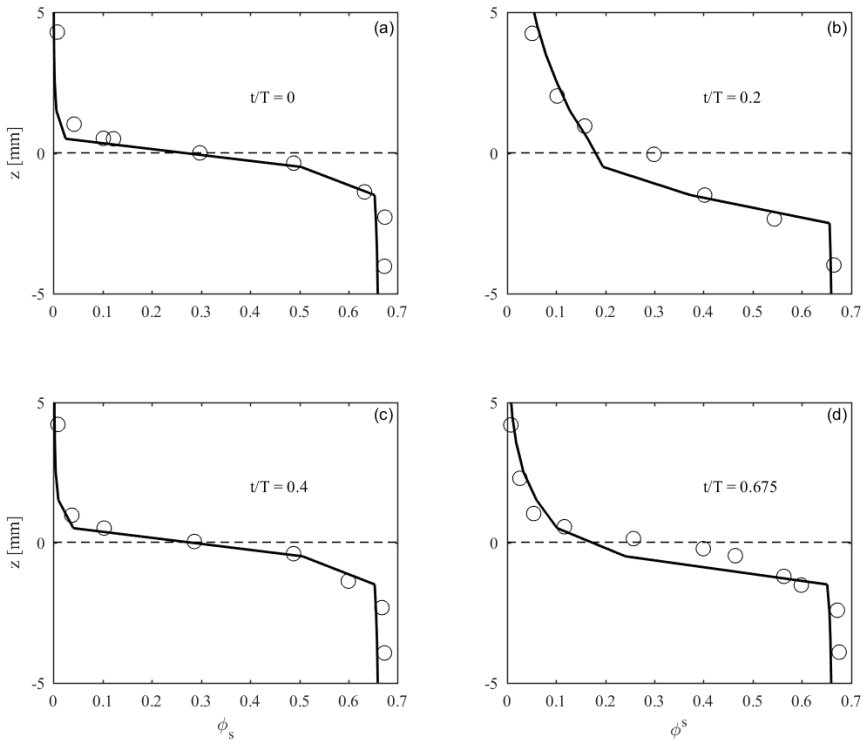

Figure 7. Instantaneous sediment concentration profiles of measured data (symbols) and model results (lines) at (a) t = 37.7 s (flow reversal), (b) t = 39 s (crest), (c) t = 40.3 s (flow reversal), and (d) t = 42.1 s (trough).

The asymmetry in the sheet layer thickness is more clearly observed in the time series of sediment concentration at the different vertical elevations (Figure 8). The numerical resolution in the vertical direction is 1 mm, hence the modeled results were linearly interpolated for comparison with measured data. Negligible erosion was observed at $z = -4$ mm in both measured data and model results, indicating no sand transport below that level (still bed level). In the pick-up layer (from $z = -4$ to 0 mm), the model results under-predict the sediment erosion at $z = -1.4$ mm. Overall, the numerical model (Figure 8b) is able to produce measured temporal evolution of sediment concentration in the sheet layer reasonably well.

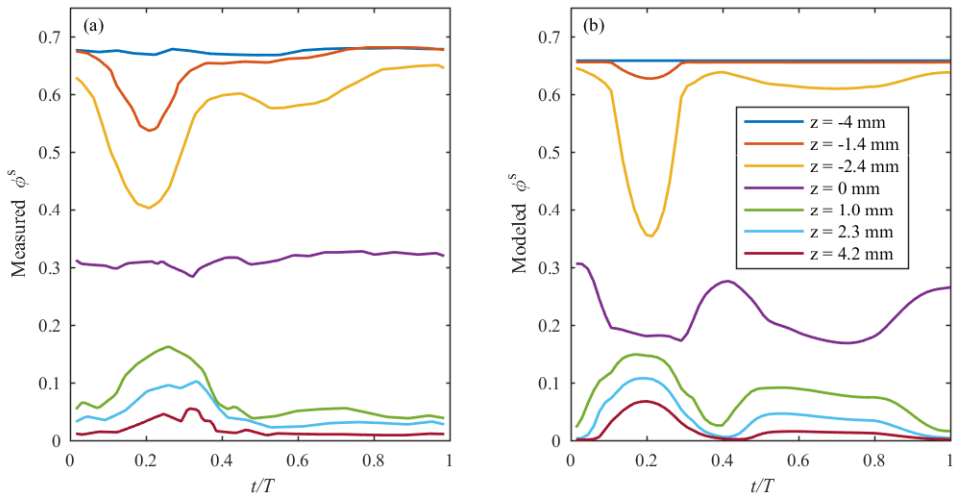

Figure 8. Comparison between (a) measured and (b) modeled sediment concentration time series at different elevations in the sheet flow layer.

Time series of net transport rate ($q^s = \int u^s \phi^s dz$) is calculated by integrating the sediment fluxes over the water column at a given instant (Figure 9). The onshore-directed sediment transport is evident under the wave crest, while offshore transport with smaller magnitude occurs during the wave trough. The results are consistent with the more significant sediment suspension under the wave crest (Figure 8). Notably reduced onshore transport during the wave crest passage was observed for the 1DV simulation using SedFoam (Figure 5; similar to OWT setup). This finding suggests that the surface wave effect, probably due to boundary layer streaming, plays an important role in driving onshore sediment transport. The wave-averaged net transport rates, $Q^s = 1/T \iint u^s \phi^s dz dt$, over the 5th wave cycle obtained from SedWaveFoam is 54 mm^2/s, which is similar to measured data of 42.9 mm^2/s using bed level change (MTA) and 70.7 mm^2/s using sediment flux (CCM and ABS). But these values are significantly larger than the 1DV SedFoam results of 35 mm^2/s.

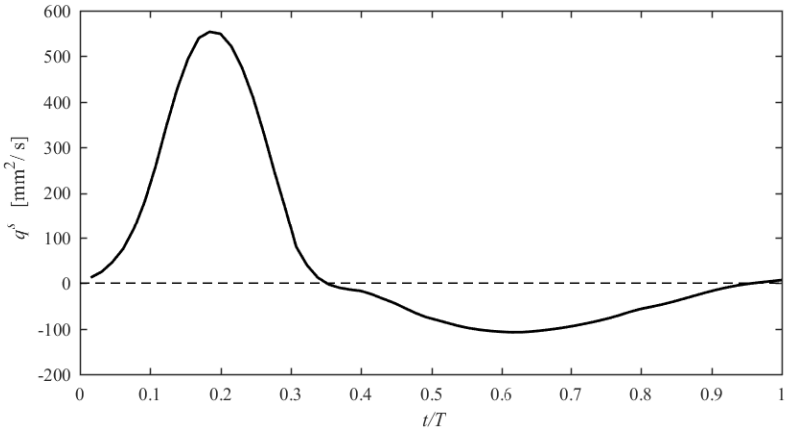

Figure 9. Time series of net transport rate in 5th wave cycle obtained from SedWaveFoam.

4. Conclusions and Future Works

A multi-phase Eulerian model for sediment transport under surface waves, SedWaveFoam, is developed by merging SedFoam with InterFoam and waves2Foam. Each model is capable in resolving sheet flow sediment transport in OWTs (O'Donoghue and Wright, 2004) and wave propagation over a barred beach (Mieras et al., *in review*). The coupled model SedWaveFoam follows the mathematical formulations for the water-sediment interactions (Cheng et al., 2017) and for the interface tracking of two impressible fluids (Jacobson et al., 2011; Klostermann et al., 2012).

Newly developed SedWaveFoam is first validated with laboratory data of Dohmen-Janssen and Hanes (2002) for sand transport in sheet flow condition under monochromatic non-breaking waves. The concurrence between modeled and measured data shows the potential of the model to investigate a wide range of sediment transport processes under realistic surface waves. The numerical model predicts the sheet flow characteristics in the concentrated region reasonably well. However, the agreement in the dilute region is less satisfactory. Through numerical experiments, it is found that surface wave effects drive more onshore transport compared to that obtained in the OWT. Higher resolution run and more detailed analysis is warranted to quantify the mechanisms responsible for the enhanced onshore transport under surface waves. SedWaveFoam has been used to simulate the case reported in the BARSED experiment (Anderson et al., *in review*; Mieras et al., *in review*). The wave steepness during BARSED was larger than those reported in Dohmen-Janssen and Hanes (2002) and simulation results can be further used to quantify boundary layer streaming and large horizontal pressure gradient associated with the steep waves.

Acknowledgements

This study is supported by NSF (OCE-1356855; OCE-1635151) of USA. Numerical simulations presented in this study were carried out using the Mills cluster at University of Delaware, and the SuperMic cluster at Louisiana State University via XSEDE (TG-OCE100015).

References

Anderson, D., Cox, D.T., Mieras, R.S., Puleo, J.A., and Hsu, T.-J,, *in review*. Observations of wave-induced pore pressure gradients and bed level response on a surf zone sandbar. *J. Geophys. Res. Oceans.*

Berberovic´, E., van Hinsberg, N. P., Jakirlic´, S., Roisman, I. V., and Tropea, C., 2009. Drop impact onto a liquid layer of finite thickness: Dynamics of the cavity evolution, *Phys. Rev.*, E79, 036306.

Cheng, Z., Hsu, T.-J. and Calantoni, J., 2017. SedFoam: A multi-dimensional Eulerian two-phase model for sediment transport and its application to momentary bed failure, *Coastal Eng*., 119, 32-50.

Dohmen-Janssen, and Hanes, D. M., 2002. Sheet flow dynamics under monochromatic nonbreaking waves, *J. Geophys. Res*., 107(C10), 3,149.

Dohmen-Janssen, C. M., Hassan, W. N., and Ribberink, J. S., 2001. Mobile effects in oscillatory sheet flow, *J. Geophys. Res*., 106(C11), 27,103-27,115.

Dong, P., and Zhang, K., 2002. Intense near-bed sediment motions in waves and currents, *Coast. Eng.,* 45(2), 75-87.

Foster, D. L., Bowen, A. J., Holman, R. A., and Natoo, P., 2006. Field evidence of pressure gradient induced incipient motion, *J. Geophys. Res*., 111, C05004.

Henderson, S. M., Allen, J. S., and Newberger, P. A., 2004. Nearshore sandbar migration predicted by an eddy-diffusive boundary layer model, *J. Geophys. Res*., 109, C06024.

Hirt, C. W., and Nichols B. D., 1981. Volume of fluid (VOF) method for the dynamics of free boundaries, *J. Comput. Phys*., 39, 201-225.

Horikawa, K., Watanabe, A., and Katori, S., 1982. A laboratory study on suspended sediment due to wave action. *Proc. 18th Int. Conf. Coast. Eng*., ASCE, Cape Town.

Hsu, T.-J., Jenkins, J. T., Liu, P. L.-F., 2004. On two-phase sediment transport: sheet flow of massive particles, Proc. R. Soc. London Ser. A Math. Phys. Eng. Sci, .460(2048), 2223-2250.

Jacobsen, N. G., Fuhrman D. R., and Fredsøe J., 2011. A wave generation toolbox for the open-source CFD library: OpenFoam®, *Int. J. Numer. Methods Fluids*, 70(9), 1073-1088.

Jacobsen, N. G., Fredsøe, J., and Jensen, J. H., 2014. Formation and development of a breaker bar under regular waves. Part 1: Model description and hydrodynamics, *Coastal Eng*., 88, 182-193.

Klostermann, J., Schaake, K., and Schwarze, R., 2012. Numerical simulation of a single rising bubble by VOF with surface compression, *Int. J. Numer. Methods Fluids*, 71(8), 960-982.

Madsen, O. S., 1974. Stability of a sand bed under breaking waves, *Proc. 14th Int. Conf. Coast. Eng*., ASCE, Reston, Va.

McLean, S. R., Ribberink, J. S., Dohmen-Janssen, C. M., and Hassan, W. N., 2001. Sand transport in oscillatory sheet flow with mean current, *J. Waterw. Port Coast. Ocean Eng.*, ASCE, 127(3), 141-151.

Meyer-Peter, E., and Müller, R., 1948. Formulas for bed-load transport, *Proc. 2nd Congress of the Int. Ass. Hydraulic Structures Res.,* Stockholm

Mieras, R., Puleo, J. A., Anderson, D., Cox, D. T., and Hsu, T. -J., 2017. Large-scale experimental observations of wave-induced sediment transport over a surf zone sandbar, *Proc. 18th Int. Conf. Coast. Dyn*., Helsingør, Denmark.

Mieras, R., Puleo, J. A., Anderson, D., Cox, D. T., and Hsu, T. -J., *in review*. Large-scale experimental observations of sheet flow on a sandbar under skewed-asymmetric waves, *J. Geophys. Res: Oceans*.

Nielsen, P., 2006. Sheet flow sediment transport under waves with acceleration skewness and boundary layer streaming, *Coastal Eng*., 53, 749-758.

Nielsen, P., and Callaghan, D. P., 2003. Shear stress and sediment transport calculations for sheet flow under waves, *Coastal Eng*., 47, 347-354.

O'Donoghue, T., Wright, S., 2004. Concentrations in oscillatory sheet flow for well sorted and graded sands, *Coast. Eng.*, 50(3), 117-138.

Ribberink, J. S., 1998. Bed-load transport for steady flows and unsteady oscillatory flows, *Coastal Eng*., 34, 59-82.

Ribberink, J. S., and Al-Salem, A. A., 1994. Sediment transport in oscillatory boundary layers in cases of rippled bed and sheet-flow, *J. Geophys. Res*., 99, 12,707-12,727.

Ruessink, B. G., van den Berg, T. J. J., and van Rijn, L. C., 2009. Modeling sediment transport beneath skewed asymmetric waves above a plane bed, *J. Geophys. Res*., 114, C11021.

Sleath, J. F. A., 1999. Conditions for plug formation in oscillatory flow, *Cont. Shelf Res*., 19(13), 1,643-1,664.

Van der A., D. A., Ribberink, J. S., van der Werf, J. J., O'Donoghue, T., Buijsrogge, R. H., and Kranenburg, W. M., 2013. Practical sand transport formula for non-breaking waves and currents, *Coastal Eng*., 76, 26-42.

Yu, X., Hsu, T.-J., and Hanes, D. M., 2010. Sediment transport under wave groups: Relative importance between nonlinear waveshape and nonlinear boundary layer streaming, *J. Geophys. Res*., 115, C02013.